ORAI1 Ca^{2+} Channels Control Endothelin-1-Induced Mitogenesis and Melanogenesis in Primary Human Melanocytes

Hedwig Stanisz[1], Alexandra Stark[1], Tatiana Kilch[2], Eva C. Schwarz[2], Cornelia S.L. Müller[1], Christine Peinelt[2], Markus Hoth[2], Barbara A. Niemeyer[2], Thomas Vogt[1] and Ivan Bogeski[2]

UV radiation of the skin triggers keratinocytes to secrete endothelin-1 (ET-1) that binds to endothelin receptors on neighboring melanocytes. Melanocytes respond with a prolonged increase in intracellular Ca^{2+} concentration ($[Ca^{2+}]_i$), which is necessary for proliferation and melanogenesis. A major fraction of the Ca^{2+} signal is caused by entry through Ca^{2+}-permeable channels of unknown identity in the plasma membrane. ORAI Ca^{2+} channels are molecular determinants of Ca^{2+} release-activated Ca^{2+} (CRAC) channels and are expressed in many tissues. Here, we show that ORAI1–3 and their activating partners stromal interaction molecules 1 and 2 (STIM1 and STIM2) are expressed in human melanocytes. Although ORAI1 is the predominant ORAI isoform, STIM2 mRNA expression exceeds STIM1. Inhibition of ORAI1 by 2-aminoethoxydiphenyl borate (2-APB) or downregulation of ORAI1 by small interfering RNA (siRNA) reduced Ca^{2+} entry and CRAC current amplitudes in activated melanocytes. In addition, suppression of ORAI1 caused reduction in the ET-1-induced cellular viability, melanin synthesis, and tyrosinase activity. Our results imply a role for ORAI1 channels in skin pigmentation and their potential involvement in UV-induced stress responses of the human skin.

Journal of Investigative Dermatology advance online publication, 9 February 2012; doi:10.1038/jid.2011.478

INTRODUCTION

Endothelin-1 (ET-1) and its two isoforms, endothelin-2 and endothelin-3, exert their biological actions through engagement of the two G-protein–coupled receptors, ET-A and ET-B. ET-1 was first isolated from vascular endothelial cells and characterized as a potent vasoconstrictor (Yanagisawa *et al.*, 1988). Besides its essential function in the cardiovascular system, a role for ET-1 has been described in the physiology and pathophysiology of the renal, central nervous, gastrointestinal, and immune systems (Rubanyi and Polokoff, 1994; Levin, 1995; Watts, 2010). In the skin, ET-1 is secreted from keratinocytes following their exposure to UV radiation and affects neighboring melanocytes through activation of their ET-B receptors (Yada *et al.*, 1991; Imokawa *et al.*, 1992, 1995; Hirobe, 2011). Furthermore, it has been suggested that ET-1 has anti-apoptotic effects and reduces DNA damage in human melanocytes (Kadekaro *et al.*, 2005).

Activation of ET-B receptors leads to phospholipase C–dependent formation of IP_3 and diacylglycerol (Kang *et al.*, 1998; Slominski *et al.*, 2004). IP_3 triggers the IP_3 receptors on the endoplasmic reticulum (ER) and causes transient depletion of ER Ca^{2+} stores. Reduction in ER Ca^{2+} is sensed by two ER-based proteins, stromal interaction molecules 1 and 2 (STIM1 and STIM2) (Liou *et al.*, 2005; Zhang *et al.*, 2005), that then oligomerize and translocate toward the plasma membrane where they activate Ca^{2+} release-activated Ca^{2+} (CRAC) channels encoded by the *ORAI* genes (Feske *et al.*, 2006; Vig *et al.*, 2006; Zhang *et al.*, 2006). ORAI1 and its homologs ORAI2 and ORAI3 are highly selective Ca^{2+} channels with cytosolic N- and C-termini and four transmembrane segments. The signaling pathway leading to ORAI activation is also known as store-operated Ca^{2+} entry (Parekh and Putney, 2005), whereas the ion current conducted by CRAC/ORAI channels is known as I_{CRAC} (Hoth and Penner, 1992).

Concomitant production of diacylglycerol together with a rise in $[Ca^{2+}]_i$ activate protein kinases that via phosphorylation of Raf-1 activate mitogen-activated protein kinase signaling pathways and CRE-binding protein-dependent phosphorylation of microphthalmia-associated transcription

[1]*Department of Dermatology, Venerology and Allergology, University Hospital of the Saarland, Homburg, Germany and* [2]*Department of Biophysics, School of Medicine, Saarland University, Homburg, Germany*

Correspondence: Hedwig Stanisz, Department of Dermatology, Venerology and Allergology, University Hospital of the Saarland, Homburg, Germany. E-mail: hedwig.stanisz@uks.eu; Ivan Bogeski, Department of Biophysics, Geb. 58, School of Medicine, Saarland University, 66421 Homburg, Germany. E-mail: ivan.bogeski@uks.eu

Abbreviations: 2-APB, 2-aminoethoxydiphenyl borate; CRAC, Ca^{2+} release-activated Ca^{2+}; ER, endoplasmic reticulum; ET-1, endothelin-1; siRNA, small interfering RNA; STIM, stromal interaction molecule; TBP, TATA-binding protein

Received 8 September 2011; revised 25 November 2011; accepted 2 December 2011

factor and its subsequent upregulation (Imokawa *et al.*, 2000; Sato-Jin *et al.*, 2008). Microphthalmia-associated transcription factor regulates the expression of multiple genes involved in melanogenesis and melanocyte survival such as tyrosinase, TRP1 and 2, Bcl2, and CDK2 (Slominski *et al.*, 2004; Sato-Jin *et al.*, 2008).

Changes in $[Ca^{2+}]_i$ are thus important determinants for proper melanocyte function (Schallreuter *et al.*, 2008). High $[Ca^{2+}]_i$ is also required for active transport of L-phenylalanine into melanocytes by the calmodulin-dependent Ca^{2+}-ATPase as well as for its turnover to L-tyrosine, an essential signaling event in melanin synthesis (Schallreuter and Wood, 1999; Schallreuter *et al.*, 2008). Furthermore, it has been shown that melanin binds Ca^{2+} and thereby regulates the redox state of melanocytes to prevent cell damage by oxidative stress (Hoogduijn *et al.*, 2004). In addition, ET-1-induced phosphorylation of CRE-binding protein as well as the scaffold protein kinase suppressor of Ras (KSR2) activation of ERK cascade are Ca^{2+}-dependent processes (Tada *et al.*, 2002; Dougherty *et al.*, 2009). In pathophysiological situations, increases in $[Ca^{2+}]_i$ have been implicated in melanoma growth and tumor invasion (Somlyo and Somlyo, 2003; Feldman *et al.*, 2010; Arozarena *et al.*, 2011). Interestingly, before the discovery of STIM1 as a CRAC channel activator, it was shown that STIM1 is upregulated in metastatic melanomas and can serve as a metastatic marker (Suyama *et al.*, 2004).

Despite the established importance of Ca^{2+} for proper melanocyte function, the molecular identity of the major players involved in regulation of the Ca^{2+} homeostasis have not been fully elucidated. More information is available on Ca^{2+} homeostasis in melanoma cells (Schallreuter *et al.*, 1992; Nilius *et al.*, 1993; Allen *et al.*, 1997; Deli *et al.*, 2007).

It has been proposed that TRP channels such as TRPM1 are responsible for Ca^{2+} influx across the plasma membrane and thus regulate melanin production in human melanocytes (Devi *et al.*, 2009; Oancea *et al.*, 2009). However, TRPM1 channels are not store operated and will probably not be activated by ET-1-induced IP_3 production. At present, nothing is known about the functional role of ORAI channels and their activators STIM1 and 2 in human melanocytes.

RESULTS

To examine a potential role of ORAI channels in melanocytes, we analyzed $[Ca^{2+}]_i$ following the application of different stimuli. Melanocytes were exposed to nominally Ca^{2+}-free bath solution and treated with 10 nM ET-1 (Figure 1a). This led to a rapid and transient increase in $[Ca^{2+}]_i$, because of depletion of intracellular ER Ca^{2+} stores. Addition of Ca^{2+} to the external buffer after $[Ca^{2+}]_i$ had returned to basal levels caused a rapid influx of Ca^{2+} (7.2 ± 0.6 nM s^{-1}), reaching an average maximal amplitude of ~612 nM that then slowly declines. Similarly, addition of 1 μM thapsigargin to Ca^{2+}-free bath solution induced a transient increase in $[Ca^{2+}]_i$ because of nonreversible inhibition of the sarco/ER Ca^{2+}-ATPases activity and a subsequent more sustained external Ca^{2+} influx upon Ca^{2+} addition (Figure 1b). The Ca^{2+}-influx rate was 7.04 ± 1.4 nM s^{-1}, resulting in an average maximal $[Ca^{2+}]_i$ of ~540 nM. To test a potential contribution of ORAI channels

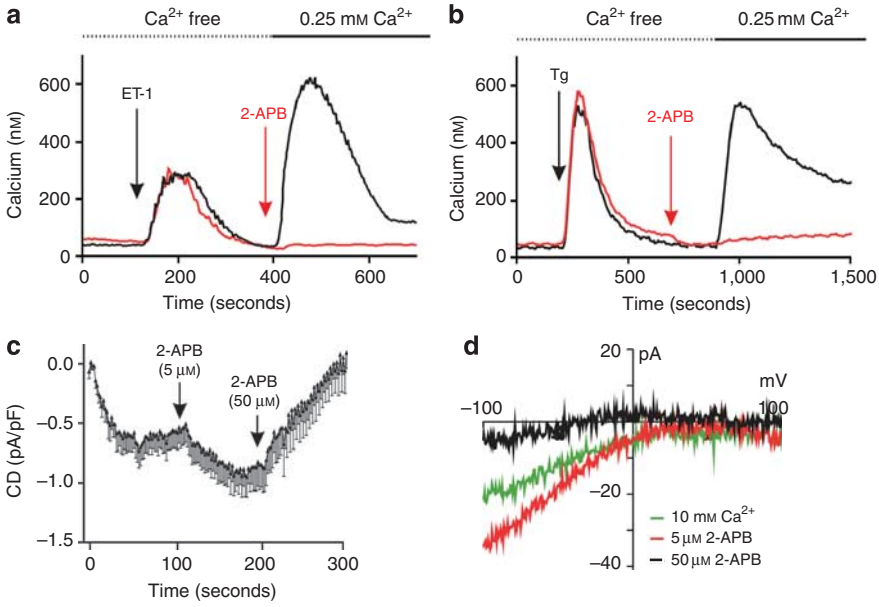

Figure 1. Characterization of melanocyte store-operated Ca^{2+} entry (SOCE) and I_{CRAC}. (**a**) Endothelin-1 (ET-1; 10 nM)-induced $[Ca^{2+}]_i$ signals in melanocytes without 2-aminoethoxydiphenyl borate (2-APB; black trace, $n = 50$) or with 50 μM 2-APB (red, $n = 74$) in Ca^{2+}-free and 0.25 mM Ca^{2+}-containing external bath solution. CRAC, Ca^{2+} release-activated Ca^{2+}. (**b**) Intracellular $[Ca^{2+}]_i$ in melanocytes before and after addition of 1 μM thapsigargin (Tg), without 2-APB (black trace, $n = 11$) or with 50 μM 2-APB (red, $n = 23$) in Ca^{2+}-free and 0.25 mM Ca^{2+}-containing external bath solution. (**c**) Average I_{CRAC} current densities (CDs) at –80 mV in 10 mM Ca^{2+}-containing external bath solution in primary human melanocytes. 2-APB (5 μM) was added 100 seconds after break-in whereas 50 μM 2-APB was added after 200 seconds ($n = 9$). Error bars indicate means ± SEM. (**d**) Voltage/current (I/V) relationship in the absence (green) or with 5 μM 2-APB (red) or 50 μM 2-APB (black); $n = 9$.

during Ca^{2+} influx, we applied 2-aminoethoxydiphenyl borate (2-APB), an inhibitor of ORAI1 and ORAI2 channels. As depicted in Figure 1a and b (red traces), 50 μM 2-APB abolished both the ET-1 and the thapsigargin-induced increase in $[Ca^{2+}]_i$, indicating a role of ORAI1 or ORAI2 in ET-1-triggered melanocyte store-operated Ca^{2+} entry.

If ORAI1 or ORAI2 are involved in Ca^{2+} entry in melanocytes, CRAC currents should be recordable. Using the whole-cell patch-clamp configuration, we analyzed currents following Ca^{2+} store depletion with 50 μM IP_3 in the patch pipette. As shown in Figure 1c, melanocytes responded with rapidly activating inward currents that reached a steady state of 0.61 ± 0.12 pA/pF after 50 seconds. In line with the known pharmacological properties of I_{CRAC}, current densities were facilitated by low (5 μM) 2-APB concentrations and inhibited by 50 μM 2-APB (Prakriya and Lewis, 2001). Furthermore, the current/voltage (I/V) relationship showed typical inwardly rectifying properties as expected of I_{CRAC} (Figure 1d). To characterize the molecular composition of CRAC channels in more detail, we evaluated the relative expression levels of ORAI and STIM isoforms with quantitative real-time PCR (Figure 2a). Cq values were normalized to the reference gene TATA-binding protein (TBP). Figure 2a shows that ORAI1 is the most abundant ORAI isoform in melanocytes. Interestingly, STIM2 mRNA is higher than STIM1, which corresponds with the finding that cells originating from the neural crest express higher amounts of STIM2 than STIM1 (Berna-Erro *et al.*, 2009).

To test the contribution of ORAI1 in the ET-1-triggered Ca^{2+}-influx, we used small interfering RNA (siRNA) against ORAI1 (O1siRNA) to downregulate ORAI1 expression and performed Ca^{2+} imaging experiments. ET-1 (10 nM) evoked normal Ca^{2+} store release in control (CTRL) and O1siRNA-treated melanocytes. However, the $[Ca^{2+}]_i$ increase due to Ca^{2+} entry across the plasma membrane was significantly reduced in the cells treated with O1siRNA (Figure 2b, red trace). CTRLsiRNA-transfected melanocytes show an average maximal $[Ca^{2+}]_i$ concentration of 634 ± 30 nM, whereas O1siRNA-treated cells peak at 213 ± 9 nM ($P<0.001$). Because the initial slope of the rise in $[Ca^{2+}]_i$ directly relates to

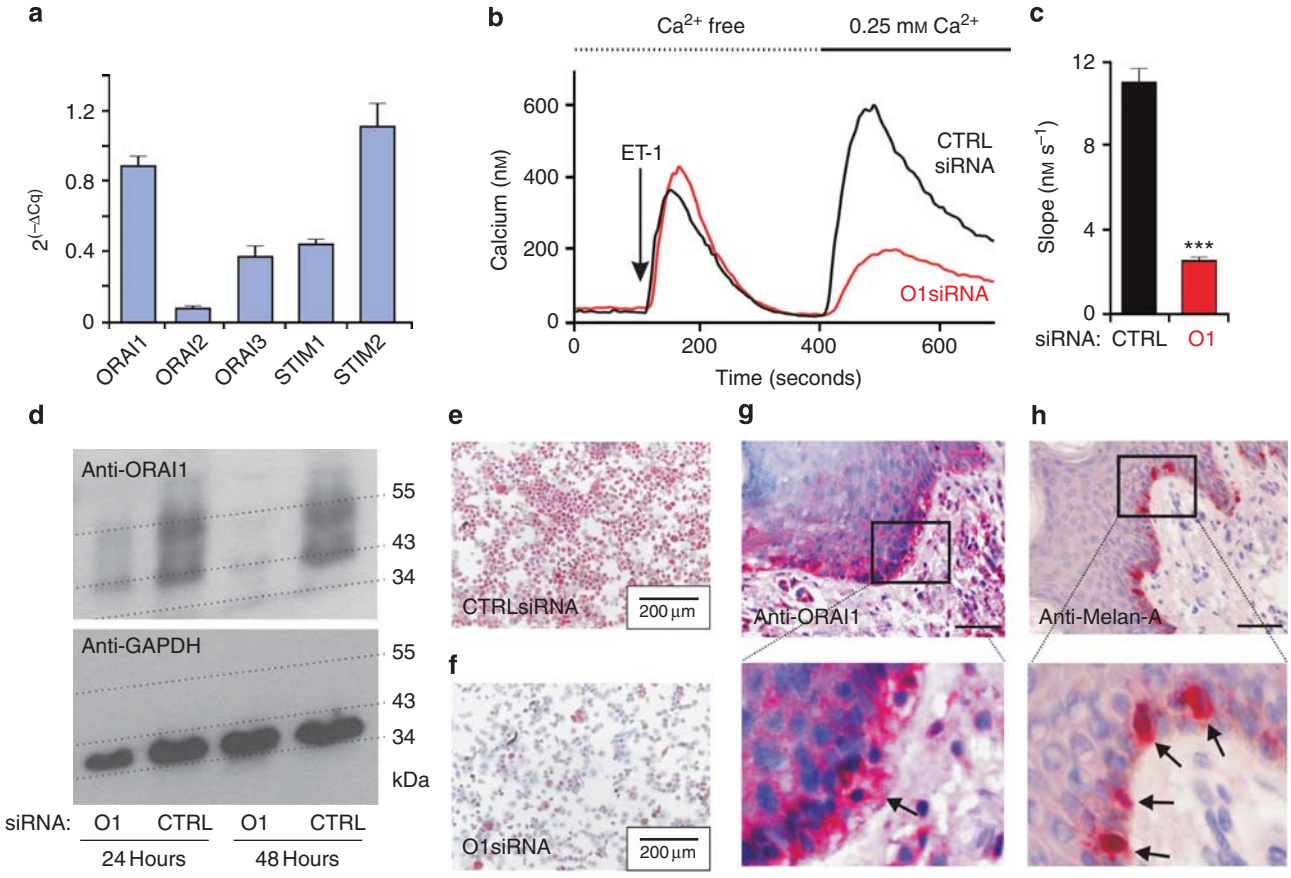

Figure 2. Expression of ORAI1–3 and stromal interaction molecules 1 and 2 (STIM1–2) in melanocytes; ORAI1 downregulation. (**a**) Quantitative real-time PCR (RT-PCR) analyses of *ORAI1–3* and *STIM1–2* expression normalized to TATA box-binding protein (TBP) in melanocytes from four healthy human donors with different pigmentation ($n=6$). (**b**) The effect of endothelin-1 (ET-1) on $[Ca^{2+}]_i$ in melanocytes treated with control small interfering RNA (CTRLsiRNA; black, $n=91$) and O1siRNA (red, $n=98$). (**c**) Ca^{2+}-influx rate calculated between 410 and 460 seconds from the traces shown in **b**. Error bars indicate means ± SEM. (**d**) Western blot analyses of ORAI1 expression in melanocytes treated with CTRL and O1siRNA at 24 and 48 hours after transfection. (**e, f**) ORAI1 expression in melanocyte cytospins treated with CTRL or O1siRNA. Bar = 200 μm. (**g, h**) Immunohistochemical staining of (**g**) ORAI1 and (**h**) melan-A in healthy human foreskin. Arrows indicate melanocytes in the basal epidermal layer. Bar = 50 μm. GAPDH, glyceraldehyde-3-phosphate dehydrogenase. ***$P < 0.001$.

the activity of the influx channels, we analyzed the Ca^{2+}-influx rate during the first 50 seconds following Ca^{2+} addition and confirmed a highly significant 77% decrease also in the Ca^{2+}-influx rate (Figure 2c). To verify the efficiency of siRNA treatment, we performed western blot analysis of cells transfected with CTRL and O1siRNA. Cells were lysed 24 or 48 hours after transfection. Because ORAI1 is a complex glycosylated protein, it exists in several molecular weight forms: a theoretical molecular weight of 32.7 kDa of the unmodified protein and two major glycosylated proteins of ~43 kDa and ~50 kDa (Figure 2d, CTRL-transfected cells). ORAI1 protein expression was strongly reduced 24 and 48 hours after siRNA transfection, thus confirming antibody specificity, with the control protein glyceraldehyde-3-phosphate dehydrogenase (GAPDH) not being affected by the O1siRNA (Figure 2d). In addition, we performed immunohistochemical analyses of primary melanocytes transfected with either CTRL or O1siRNA, confirming expression of ORAI1 and its successful downregulation by siRNA treatment (Figure 2e and f). Furthermore, to examine ORAI1 expression not only in cultured melanocytes but also *in vivo*, we performed immunohistochemical analyses on samples from healthy human foreskin (Figure 2g). The stains indicate abundant presence of ORAI1 in melanocytes at the basal epidermal layer as well as in all other epidermal cells, confirming the finding that keratinocytes also express ORAI1 (see McCarl *et al.*, 2009). To verify the presence of melanocytes in the basal epidermal layer, we stained for melan-A in subsequent sections of the same foreskin sample (Figure 2h).

Because ET-1 serves as a mitogenic and melanogenic stimulus for melanocytes (Yada *et al.*, 1991; Imokawa *et al.*, 1992, 1995), we investigated the potential role of ORAI1 in melanocyte viability (metabolic activity). As the melanocyte growth medium contains several mitogenic stimuli that could interfere with determining the effect of ET-1 (see Table 1 and Materials and Methods for details), we transferred melanocytes into three media with different or without supplementation (Table 1) for at least 48 hours before stimulation with ET-1. Three concentrations of ET-1 (0.1, 1, and 10 nM) were used and viability was determined at 3, 24, and 48 hours after addition of ET-1. Figure 3a–c shows a clear concentration- and time-dependent increase in viability in ET-1-stimulated cells compared with control cells without ET-1 added to the nonsupplemented medium (−/−). After 3 hours, no significant change in viability was observed in cells exposed to ET-1 (0.1–10 nM) in comparison with those without stimulus (Figure 3a). However, after 24 hours with ET-1 stimulation, 1 and 10 nM ET-1-induced a 54 and 141% increase in viability compared with nonstimulated cells (Figure 3b). After 48 hours, this effect becomes even more prominent with an increase of 30% in 0.1 nM, 110% in 1 nM, and 257% in 10 nM ET-1-stimulated cells (Figure 3c). The ET-1-induced increase in viability is also observed in supplemented media, although the effects are smaller (Supplementary Figure S1a-c online).

Given that ET-1 mediates Ca^{2+}-influx mainly through ORAI1 channels, we determined the role of ORAI1 in this ET-1-induced increase in viability. Melanocytes were transfected with CTRL or O1siRNA, placed in (−/−) medium, and stimulated as before (see Figure 3a–c). To isolate the effect of ORAI1 on the ET-1-induced increase in viability, we first calculated the percent change in viability of the O1siRNA-treated cells compared with the ones treated with CTRLsiRNA and then subtracted the background values obtained from cells grown without ET-1 (Figure 3d–f). After 24 and 48 hours, both CTRL and O1siRNA melanocytes showed increased viability upon ET-1 treatment. However, the ET-1-induced increase in viability was significantly lower in cells with reduced levels of ORAI1 (Figure 3d–f). At 24 hours, the ET-1-induced increase in viability was reduced by 83% (0.1 nM), 57% (1 nM), and 68% (10 nM) in O1siRNA-treated melanocytes versus CTRLsiRNA-treated ones (Figure 3e). After 48 hours, the reduction of the ET-1-induced increase in viability was 92%, 72%, and 47%, respectively (Figure 3f). These findings clearly indicate that ORAI1 plays a significant role in the ET-1-induced melanocyte viability. In medium with reduced supplements (−/+), similar patterns between CTRL and O1siRNA cells could be observed despite the reduced effect of ET-1. In medium with complete supplementation (+/+), however, the effect of ET-1 on melanocyte viability was almost negligible, thus not allowing evaluation of the siRNA treatment (Supplementary Figure S1d-i online).

Because melanin production is one of the most important physiological functions of melanocytes, we asked whether the ET-1/ORAI1 pathway is involved in melanogenesis. To avoid interference of other pro-melanotic compounds present in the (+/+) medium, cells were first kept in (−/+) medium for 7 days and for 2 subsequent days in (−/−) medium. Cells were then stimulated with 10 nM ET-1 in the presence or absence of 50 μM 2-APB. Melanin content was measured after 48 hours and its concentration was calculated using a calibration curve with known melanin concentrations. Figure 4a shows that the basal melanin concentration in nontreated cells was 20.7 ± 1.13 pM per cell. Treatment with 2-APB alone did not induce significant changes in melanin content. However, after 48 hours in the presence of 10 nM

Table 1. Differently supplemented growth media used in this study

M2 growth medium without supplement (−/−)	Only medium
M2 growth medium with reduced supplements (−/+)	Medium+insulin+hydrocortisone+BFGF
M2 growth medium with complete supplements (+/+)	Medium+insulin+hydrocortisone+BFGF+BPE+PMA

Insulin (5 μg ml^{-1}), hydrocortisone (0.5 μg ml^{-1}), basic fibroblast growth factor (BFGF; 1 ng ml^{-1}), bovine pituitary extract (BPE; 0.4%), and phorbol 12-myristate 13-acetate (PMA; 175 nM).

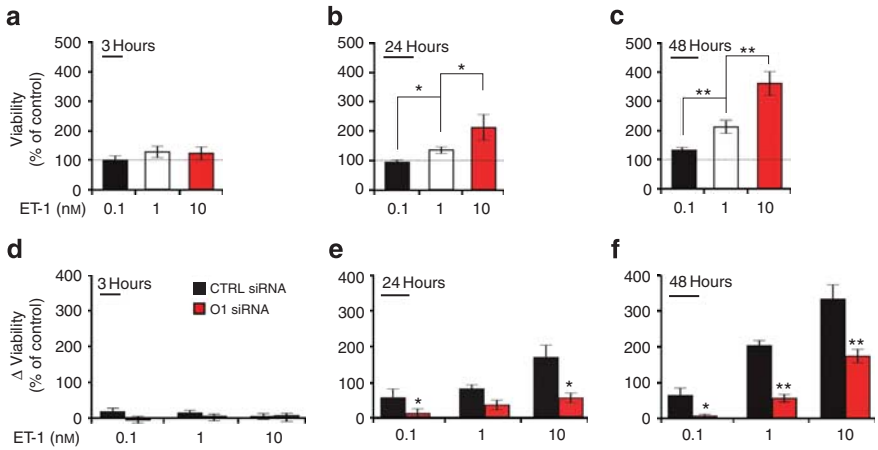

Figure 3. The role of ORAI1 in endothelin-1 (ET-1)-induced increase in melanocyte viability. (**a–c**) Relative melanocyte viability in supplement-free medium (−/−) (**a**) 3 hours, (**b**) 24 hours, and (**c**) 48 hours after stimulation with 0.1, 1, and 10 nM ET-1; $n = 5$. Results are presented as percent of control (100%, without ET-1). (**d–f**) Change in the ET-1-induced increase in viability of melanocytes treated with control (CTRL; black) or O1siRNA (red) in supplement-free medium (−/−) (**d**) 3 hours, (**e**) 24 hours, and (**f**) 48 hours after stimulation with 0.1, 1, and 10 nM ET-1; $n = 7$. siRNA, small interfering RNA. Measurements with ET-1 were evaluated as percent of control (100%, without ET-1). To isolate the effect of ORAI1 on ET-1-induced increase in viability, 100% (value without ET-1) was subtracted from all values in **d–f**. Error bars indicate means ± SEM. $^*P < 0.05$ and $^{**}P < 0.01$.

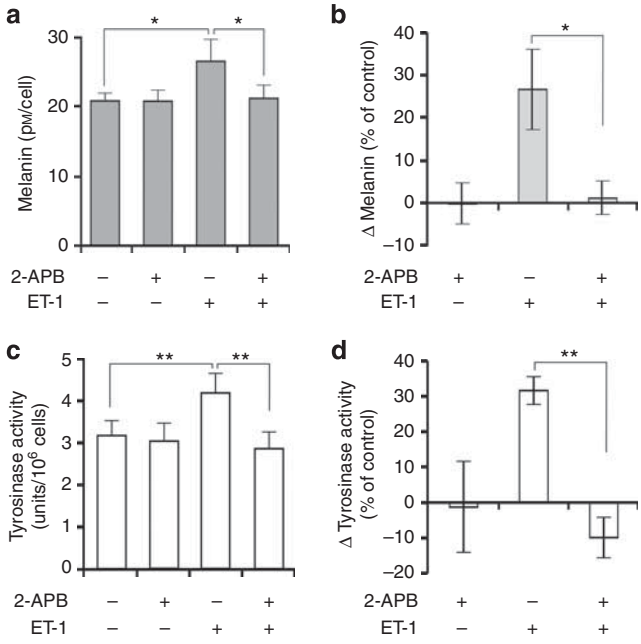

Figure 4. The role of ORAI1 in endothelin-1 (ET-1)-induced melanin production and tyrosinase activity. Melanin amount and tyrosinase activity in melanocytes grown in (−/+) medium for 7 days and in (−/−) medium for 3 days before stimulation. (**a**) Cells were stimulated with 10 nM ET-1 in the presence or absence of 50 μM 2-aminoethoxydiphenyl borate (2-APB). Melanin content was measured 48 hours after stimulation; $n = 4$. (**b**) Quantification of results shown in **a**. (**c**) Tyrosinase activity 6 hours after ET-1 and 2-APB stimulation; $n = 6$. (**d**) Quantification of results shown in **c**. In **b** and **d** the effects of ET-1 and 2-APB are evaluated as percent of control (100%, without ET-1). To isolate the effect of ORAI1 on ET-1-induced melanogenesis, 100% was subtracted from all values. Error bars indicate means ± SEM. $^*P < 0.05$ and $^{**}P < 0.01$.

ET-1, the melanin concentration in melanocytes was significantly increased to 26.5 ± 3.2 pM per cell. This increase was suppressed in cells that were additionally treated with 2-APB (Figure 4a). To further quantify the results shown in Figure 4a, we calculated the percent of change in ET-1- and/or 2-APB-treated cells and found that the ET-1-induced increase in melanin concentration was 26.6 ± 9.4% compared with untreated cells (Figure 4b). However, augmented melanin levels could be due to either increased synthesis or decreased secretion. To address this, we performed measurements of tyrosinase activity. Tyrosinase is one of the key enzymes in the melanin biosynthetic pathway and its activity is coupled with synthesis and not secretion. Melanocytes were pretreated in the same manner as for melanin measurements and were stimulated with ET-1 and/or 2-APB for 6 hours. Figure 4c shows that ET-1 treatment induced significantly higher tyrosinase activity (4.18 ± 0.47 vs. 3.17 ± 0.36 U per 10^6 cells) that was blocked by ORAI1 inhibitor 2-APB (2.86 ± 0.39 U per 10^6 cells). Quantification of the results in Figure 4c indicates that ET-1-induced a 32 ± 4% increase in tyrosinase activity when compared with controls. This increase is comparable to the increase in melanin (26.6%).

In summary, our findings suggest that Ca^{2+} influx controlled by ORAI1 channels not only mediates the mitogenic effects of ET-1, but is also involved in the regulation of ET-1-regulated melanogenesis in human melanocytes.

DISCUSSION

Our results show that ORAI1 channels are one of the major Ca^{2+}-entry pathways in primary human melanocytes. The expression pattern of the three ORAI isoforms and their activators STIM1 and STIM2 revealed that ORAI1 and STIM2 transcripts are most abundant. High relative expression of STIM2 may reflect the neural origins of melanocytes; however, relative expression of ORAI1 compared with ORAI2 is relatively low in neuronal cells, but high in melanocytes.

STIM2 has lower affinity for Ca^{2+} than STIM1 and may thus increase basal $[Ca^{2+}]_i$. In addition, because of the

slower oligomerization of STIM2 upon ER Ca^{2+} store depletion, cells expressing higher amounts of STIM2 should display lower but prolonged increases in $[Ca^{2+}]_i$ (Berna-Erro *et al.*, 2009). Interestingly, this seems not to be the case in melanocytes despite their high STIM2 content as thapsigargin- and ET-1-induced store-operated Ca^{2+} entry is rapid and large but returns to basal levels after relatively short time periods (Figures 1a and b). A possible explanation for these differences may be cellular morphology, size, and location of ER and mitochondria and/or the role of other STIM-regulated Ca^{2+}-permeating channels such as TRPCs and/or voltage-gated Ca^{2+} channels (CaV) (Worley *et al.*, 2007; Park *et al.*, 2010; Wang *et al.*, 2010). Further studies are needed to examine not only the role of STIM2 in melanocytes, but also the functional significance of different ORAI/TRPC/CaV/STIM expression ratios in different skin cell types.

This study assigns an important physiological role for ORAI1 in ET-1-regulated melanocyte function. Measurements of cellular viability and melanogenesis suggest that proper melanocyte function strongly depends on ORAI1. Because ET-1 is produced by keratinocytes upon UV light exposure, our results propose that ORAI1 may be involved in the process of ''adaptive tanning'' rather than in the regulation of basal skin pigmentation. A defective ORAI1-dependent Ca^{2+} entry in melanocytes may thus lead to impaired tanning ability.

Following UV radiation, keratinocytes and melanocytes, in addition to ET-1, also secret corticotropin-releasing hormone, which serves as a paracrine signal and leads to increase in the local levels of proopiomelanocortin-derived peptides such as ACTH, α-melanocyte-stimulating hormone, and endorphin (Slominski *et al.*, 2000; Zbytek *et al.*, 2006). Notably, corticotropin-releasing hormone as well as ACTH also induce IP_3 production and increase in $[Ca^{2+}]_i$ (Fazal *et al.*, 1998; Wiesner *et al.*, 2003; Slominski *et al.*, 2006), raising the distinct possibility that ORAI1-mediated Ca^{2+} influx could also be involved in the regulation of cellular functions controlled by these peptides, in particular under stress conditions such as UV radiation.

In mice lacking either *ORAI1 or STIM1*, skin pathologies such as hair loss or dermatitis have been reported (Gwack *et al.*, 2008; Oh-hora *et al.*, 2008). Furthermore, in very few human patients with nonfunctional CRAC channels due to mutations in *ORAI1* and *STIM1* genes (severe combined immunodeficiency patients), ectodermal dysplasia with anhydrosis, but no detectable pigmentation defects, was observed (McCarl *et al.*, 2009; Picard *et al.*, 2009). However, it is unknown whether UV-induced skin tanning is affected in these patients. A comparison of adaptive tanning in humans with defective ORAI and/or STIM function with healthy controls could provide further evidence for the role of ET-1 and Ca^{2+} signaling in melanocyte function.

Our results also suggest that prolonged activation or upregulation of ORAI1 and STIM proteins could play a role in pigmentary disorders and even skin cancer. This assumption is supported by reports that show that defects in ET-1 signaling cascade are connected with tumor progression and metastasis in melanoma (Demunter *et al.*, 2001; Lahav *et al.*, 2004; Spinella *et al.*, 2007) and also by reports showing upregulation of ORAI and STIM proteins in cancer growth, migration, and metastasis (Suyama *et al.*, 2004; Yang *et al.*, 2009; Feng *et al.*, 2010; Motiani *et al.*, 2010; Prevarskaya *et al.*, 2011). Considering these findings, it is possible that ORAI channels may also be involved in pathophysiological melanocyte activity and in skin cancer growth and metastasis.

MATERIALS AND METHODS

Chemicals

All chemicals were purchased from Sigma if not otherwise indicated.

Cells

Cells were isolated from neonatal foreskins of healthy individuals provided by the Department of Urology, University of Saarland, with a parental consent. To establish a monoculture of human dermal melanocytes, the isolated cell mix was cultivated in M2 growth medium (Promocell, Heidelberg, Germany) at 37 °C, 5% CO_2, and 95% humidity. Keratinocytes and fibroblasts do not grow in this medium and were thus lost during cell culture. For most experiments, growth medium with different supplements was used (see Table 1). The study adhered to the Declaration of Helsinki Principles and was approved by the local ethics committee.

siRNA transfection

A total of 1.5×10^6 cells were transfected with the same O1siRNA or CTRLsiRNA (20 μM) as in Bogeski *et al.* (2010) using nucleofector technology (Lonza, Cologne, Germany) following the manufacturer's instructions.

Fluorescence-based Ca^{2+} imaging

$[Ca^{2+}]_i$ was determined using 1 μM Fura-2-acetoxymethyl ester, as described in Bogeski *et al.* (2010). The images were analyzed using TILL Vision software (TILL Vision, Munich, Germany). The absolute intracellular Ca^{2+} concentration was calculated according to Grynkiewicz *et al.* (1985).

Electrophysiology

Recordings were performed at room temperature in the tight-seal whole-cell configuration. Patch pipettes had a final resistance of 2–3 MΩ and were coated with Sigmacote. Pipette and cell capacitance were electronically compensated before each voltage ramp with an EPC-10 patch-clamp amplifier controlled by Patchmaster software (HEKA, Lambrecht, Germany). Immediately after establishing whole-cell configuration, linear voltage ramps from −150 mV to +150 mV of 50 ms duration were applied every 2 seconds from a holding potential of 0 mV for the indicated time period. Membrane currents were sampled at 10 kHz and filtered at 2.9 kHz. For leak current correction, the ramp current before current activation was subtracted. Voltages were corrected for a liquid junction potential of −10 mV. The pipette solution contained (in mM): 120 cesium-glutamate, 3 $MgCl_2$, 20 cesium-Bapta, 10 Hepes, and 0.05 IP_3 (pH 7.2 with CsOH). The bath solution contained (in mM): 120 NaCl, 10 TEA-Cl, 2 $MgCl_2$, 10 Hepes, and glucose (pH 7.2 with NaOH).

Cell viability and proliferation

Measurements were carried out in black 96-well cell culture plates with transparent bottom (BD, Heidelberg, Germany). Each data point was measured in triplicates. Melanocytes (3,000 per well) were seeded in a total volume of 200 µl growth medium and incubated at 37 °C, 5% CO_2, and 95% humidity. After 48 hours in the different growth media (see Table 1), untransfected as well as siRNA-transfected cells were stimulated with 0.1, 1, and 10 nM ET-1 or buffer (control stimulus). Cell viability was analyzed after 3, 24, and 48 hours with CellTiter-Blue assay (Promega, Mannheim, Germany). Because of the different initial values in each growth medium, viability of melanocytes without ET-1 (control) was always taken as 100%. The effect of ET-1 stimulation was calculated as percentage of control. To isolate the effect of O1siRNA treatment on ET-1-induced increase in viability, 100% (control, no ET-1) were subtracted from all values with ET-1 stimulation.

Quantitative real-time PCR

Total RNA was isolated from 1×10^6 melanocytes from four donors. Then, 1 µg of total RNA was used for reverse transcription, and 0.5 µl complementary DNA and 300 nM primer were used with a Quanti Tect SYBR green kit (Qiagen, Hilden, Germany). PCR conditions were: 15 minutes, 94 °C; 45 cycles, 30 seconds at 94 °C; 45 seconds at 58 °C; 30 seconds at 72 °C; with a final cycle (60 seconds at 95 °C; 30 seconds at 55 °C; and 30 seconds at 95 °C) using the MX3000_ cycler (Stratagene, Waldbronn, Germany). Expression of *ORAI1-3* and *STIM1-2* was normalized to the reference gene TBP (#NM_003194). Relative expression was calculated according to the ΔCq method ($2^{-\Delta Cq}$). Cq values were determined by the MX3000 software. Following primers were used: STIM1_forw_5′-CAGAGTCTGCATGACCTTCA-3′, STIM1_rev_5′-GCTTCCTGCTTAGCAAGGTT-3′, STIM2_forw_5′-GTCTCCATTCCACCCTATCC-3′, STIM2_rev_5′-GGCTAATGATCCAGGAGGTT-3′, Orai1_forw_5′-ATGAGCCTCAACGAGCACT-3′ Orai1_rev_5′-GTGGGTAGTCGTGGTCAG-3′ Orai2_forw_5′-TGGAACTGGTCACCTCTAAC-3′ Orai2_rev_5′-GGGTACTGGTACTGCGTCT-3′, Orai3_forw_5′-GTACCGGGAGTTCGTGCA-3′, Orai3_rev_5′-GGTACTCGTGGTCACTCT-3′, TBP_forw_5′-CGGAGAGTTCTGGGATTGT-3′, TBP_rev_5′-GGTTCGTGGCTCTCTTATC-3′.

Immunoblotting

A total of 50 µg protein was separated by 15% SDS-PAGE and transferred onto nitrocellulose membranes. Anti-Orai1 antibody (2 µg ml^{-1}, O8264, Sigma) incubations were performed at 4 °C overnight, and blots were washed 3 × with Tris-buffered saline and Tween 20. Secondary antibody goat anti-rabbit 1:1,000 was applied for 1 hour at room temperature. Blot was washed 3 × with Tris-buffered saline and Tween 20. Bands were detected with Lumi-Light substrate (Roche Diagnostics, Mannheim, Germany). To assess equal loading, blots were stripped and reprobed with anti-GAPDH antibody.

Immunohistochemistry

Sections from paraffin-embedded foreskins were deparafinated and pretreated with heat-induced epitope retrieval solution (Dako Cytomation target-retrieval solution, pH 6), while cultured melanocytes (5×10^5) were attached on a coverslip using a cytospin centrifuge (Thermo Type Cytospin 4, Thermo Fisher Scientific, Schwerte, Germany). Samples were stained with 20 µg ml^{-1} anti-ORAI1 (O8264, Sigma) or anti-Melan-A (clone A103, M7196; dilution 1:100; Dako, Hamburg Germany) using Dako Autostainer Plus and Dako REAL detection system, with alkaline phosphatase/RED-conjugated anti-rabbit, anti-mouse antibody (K5005). Sections were examined by light microscopy.

Melanin measurements

Cells were grown in (−/+) medium for 7 days and transferred in (−/−) medium for additional 2 days. Following this treatment, cells were stimulated with 10 nM ET-1 in the presence or absence of 50 µM 2-APB. Untreated cells (no ET-1) were used as control. After 48 hours, cells were washed twice, harvested by trypsinization, counted, and lysed in phosphate-buffered saline with 1% Triton X-100 for 30 minutes at 4 °C. Approximately 1×10^6 cells were used per condition. The lysate was than centrifuged at 14,000*g* for 40 minutes at 4 °C. The remaining pellet was dissolved in 200 µl 1 N NaOH at 85 °C for 60 minutes. To determine the melanin content, absorbance was measured at 465 nm with a reference at 630 nm. Absolute melanin content was calculated by using a melanin calibration curve obtained by dissolving concentrations of synthetic melanin in 200 µl 1 N NaOH. Melanin concentration was normalized to cell number.

Tyrosinase activity

Melanocytes were pretreated similarly as for melanin measurements and stimulated for 6 hours. 2-APB was always applied 5 minutes before ET-1. Cells were lysed in 200 µl phosphate-buffered saline with 1% Triton X-100 for 30 minutes at 4 °C and centrifuged at 14 000*g* for 30 minutes at 4 °C. Then, 50 µl of the supernatant was mixed with phosphate-buffered saline with or without 1 mM L-DOPA to a final volume of 200 µl per well. Formation of L-DOPAchrome was recorded by measuring absorbance at 465 nm with a reference at 630 nm after 45 minutes at 37 °C. The samples without L-DOPA were taken as background and were subtracted from the measured value. Tyrosinase activity was calculated from a calibration curve obtained from known mushroom tyrosinase (Sigma, T3824) concentrations and was normalized to cell number.

Data analysis and statistics

Data were analyzed using TILL Vision (TILL Photonics), Fitmaster 2.35 (HEKA) Igor Pro (Wavemetrics, Portland, OR), and Microsoft Excel (Microsoft). Data are mean ± SEM, and asterisks indicate significance: $*P<0.05$, $**P<0.01$, and $***P<0.001$ (unpaired and/or paired two-sided Student's *t*-test). For each condition, at least three experiments were performed from at least two different donors.

CONFLICT OF INTEREST

The authors state no conflict of interest.

ACKNOWLEDGMENTS

We are very grateful to Dr Dalia Al-Ansary for critical discussions and suggestions and to Dr Rebecca Körner, Bettina Strauss, and Gertrud Schwär for their assistance. This work is supported by the AvH Foundation via the joint German-Macedonian project (DEU/1128670 to IB and MH) and by the Deutsche Forschungsgemeinschaft to IB (BO 3643/2-1), CP (PE 1478/5-1, SFB894), BAN (SFB894, NI671/3-1), and MH (SFB 894).

SUPPLEMENTARY MATERIAL

Supplementary material is linked to the online version of the paper at http://www.nature.com/jid

REFERENCES

Allen DH, Lepple-Wienhues A, Cahalan MD (1997) Ion channel phenotype of melanoma cell lines. *J Membr Biol* 155:27–34

Arozarena I, Sanchez-Laorden B, Packer L *et al.* (2011) Oncogenic BRAF induces melanoma cell invasion by downregulating the cGMP-specific phosphodiesterase PDE5A. *Cancer Cell* 19:45–57

Berna-Erro A, Braun A, Kraft R *et al.* (2009) STIM2 regulates capacitive Ca2+ entry in neurons and plays a key role in hypoxic neuronal cell death. *Sci Signal* 2:ra67

Bogeski I, Kummerow C, Al-Ansary D *et al.* (2010) Differential redox regulation of ORAI ion channels: a mechanism to tune cellular calcium signaling. *Sci Signal* 3:ra24

Deli T, Varga N Ádám A, Kenessey I *et al.* (2007) Functional genomics of calcium channels in human melanoma cells. *Int J Cancer* 121: 55–65

Demunter A, De Wolf-Peeters C, Degreef H *et al.* (2001) Expression of the endothelin-B receptor in pigment cell lesions of the skin. *Virchows Archiv* 438:485–91

Devi S, Kedlaya R, Maddodi N *et al.* (2009) Calcium homeostasis in human melanocytes: role of transient receptor potential melastatin 1 (TRPM1) and its regulation by ultraviolet light. *Am J Physiol Cell Physiol* 297:C679–87

Dougherty MK, Ritt DA, Zhou M *et al.* (2009) KSR2 is a calcineurin substrate that promotes ERK cascade activation in response to calcium signals. *Mol Cell* 34:652–62

Fazal N, Slominski A, Choudhry MA *et al.* (1998) Effect of CRF and related peptides on calcium signaling in human and rodent melanoma cells. *FEBS Lett* 435:187–90

Feldman B, Fedida-Metula S, Nita J *et al.* (2010) Coupling of mitochondria to store-operated Ca2+-signaling sustains constitutive activation of protein kinase B/Akt and augments survival of malignant melanoma cells. *Cell Calcium* 47:525–37

Feng M, Grice DM, Faddy HM *et al.* (2010) Store-independent activation of Orai1 by SPCA2 in mammary tumors. *Cell* 143:84–98

Feske S, Gwack Y, Prakriya M *et al.* (2006) A mutation in Orai1 causes immune deficiency by abrogating CRAC channel function. *Nature* 441:179–85

Grynkiewicz G, Poenie M, Tsien RY (1985) A new generation of Ca2+ indicators with greatly improved fluorescence properties. *J Biol Chem* 260:3440–50

Gwack Y, Srikanth S, Oh-hora M *et al.* (2008) Hair loss and defective T- and B-cell function in mice lacking ORAI1. *Mol Cell Biol* 28: 5209–22

Hirobe T (2011) How are proliferation and differentiation of melanocytes regulated? *Pigment Cell Melanoma Res* 24:462–78

Hoogduijn MJ, Cemeli E, Ross K *et al.* (2004) Melanin protects melanocytes and keratinocytes against H2O2-induced DNA strand breaks through its ability to bind Ca2+. *Exp Cell Res* 294:60–7

Hoth M, Penner R (1992) Depletion of intracellular calcium stores activates a calcium current in mast cells. *Nature* 355:353–6

Imokawa G, Kobayasi T, Miyagishi M (2000) Intracellular signaling mechanisms leading to synergistic effects of endothelin-1 and stem cell factor on proliferation of cultured human melanocytes. Cross-talk via trans-activation of the tyrosine kinase c-kit receptor. *J Biol Chem* 275:33321–8

Imokawa G, Miyagishi M, Yada Y (1995) Endothelin-1 as a new melanogen: coordinated expression of its gene and the tyrosinase gene in UVB-exposed human epidermis. *J Invest Dermatol* 105:32–7

Imokawa G, Yada Y, Miyagishi M (1992) Endothelins secreted from human keratinocytes are intrinsic mitogens for human melanocytes. *J Biol Chem* 267:24675–80

Kadekaro AL, Kavanagh R, Kanto H *et al.* (2005) alpha-Melanocortin and endothelin-1 activate antiapoptotic pathways and reduce DNA damage in human melanocytes. *Cancer Res* 65:4292–9

Kang H-Y, Kang W-H, Lee CO (1998) Endothelin-B receptor-mediated Ca2+ signaling in human melanocytes. *Pflügers Arch* 435:350–6

Lahav R, Suvà M-L, Rimoldi D *et al.* (2004) Endothelin receptor B inhibition triggers apoptosis and enhances angiogenesis in melanomas. *Cancer Res* 64:8945–53

Levin ER (1995) Endothelins. *N Engl J Med* 333:356–63

Liou J, Kim ML, Heo WD *et al.* (2005) STIM is a Ca2+ sensor essential for Ca2+-store-depletion-triggered Ca2+ influx. *Curr Biol* 15:1235–41

McCarl CA, Picard C, Khalil S *et al.* (2009) ORAI1 deficiency and lack of store-operated Ca2+ entry cause immunodeficiency, myopathy, and ectodermal dysplasia. *J Allergy Clin Immunol* 124:1311–8 e7

Motiani RK, Abdullaev IF, Trebak M (2010) A novel native store-operated calcium channel encoded by Orai3. *J Biol Chem* 285:19173–83

Nilius B, Schwarz G, Droogmans G (1993) Control of intracellular calcium by membrane potential in human melanoma cells. *Am J Physiol* 265:C1501–C10

Oancea E, Vriens J, Brauchi S *et al.* (2009) TRPM1 forms ion channels associated with melanin content in melanocytes. *Sci Signal* 2:ra21

Oh-hora M, Yamashita M, Hogan PG *et al.* (2008) Dual functions for the endoplasmic reticulum calcium sensors STIM1 and STIM2 in T cell activation and tolerance. *Nat Immunol* 9:432–43

Parekh AB, Putney Jr JW (2005) Store-operated calcium channels. *Physiol Rev* 85:757–810

Park CY, Shcheglovitov A, Dolmetsch R (2010) The CRAC channel activator STIM1 binds and inhibits L-Type voltage-gated calcium channels. *Science* 330:101–5

Picard C, McCarl CA, Papolos A *et al.* (2009) STIM1 mutation associated with a syndrome of immunodeficiency and autoimmunity. *N Engl J Med* 360:1971–80

Prakriya M, Lewis RS (2001) Potentiation and inhibition of Ca(2+) release-activated Ca(2+) channels by 2-aminoethyldiphenyl borate (2-APB) occurs independently of IP(3) receptors. *J Physiol* 536:3–19

Prevarskaya N, Skryma R, Shuba Y (2011) Calcium in tumour metastasis: new roles for known actors. *Nat Rev Cancer* 11:609–18

Rubanyi GM, Polokoff MA (1994) Endothelins: molecular biology, biochemistry, pharmacology, physiology, and pathophysiology. *Pharmacol Rev* 46:325–415

Sato-Jin K, Nishimura EK, Akasaka E *et al.* (2008) Epistatic connections between microphthalmia-associated transcription factor and endothelin signaling in Waardenburg syndrome and other pigmentary disorders. *FASEB J* 22:1155–68

Schallreuter KU, Kothari S, Chavan B *et al.* (2008) Regulation of melanogenesis–controversies and new concepts. *Exp Dermatol* 17:395–404

Schallreuter KU, Wood JM (1999) The importance of L-phenylalanine transport and its autocrine turnover to L-tyrosine for melanogenesis in human epidermal melanocytes. *Biochem Biophys Res Commun* 262:423–8

Schallreuter KU, Wood JM, Ehrke C *et al.* (1992) Calcium transport and regulation in human primary and metastatic melanoma. *Biochim Biophys Acta* 1160:127–33

Slominski A, Tobin DJ, Shibahara S *et al.* (2004) Melanin pigmentation in mammalian skin and its hormonal regulation. *Physiol Rev* 84: 1155–228

Slominski A, Wortsman J, Luger T *et al.* (2000) Corticotropin releasing hormone and proopiomelanocortin involvement in the cutaneous response to stress. *Physiol Rev* 80:979–1020

Slominski A, Zbytek B, Pisarchik A *et al.* (2006) CRH functions as a growth factor/cytokine in the skin. *J Cell Physiol* 206:780–91

Somlyo AP, Somlyo AV (2003) Ca2+ sensitivity of smooth muscle and nonmuscle myosin II: modulated by G proteins, kinases, and myosin phosphatase. *Physiol Rev* 83:1325–58

Spinella F, Rosanò L, Di Castro V *et al.* (2007) Endothelin-1 and endothelin-3 promote invasive behavior via hypoxia-inducible factor-1α in human melanoma cells. *Cancer Res* 67:1725–34

Suyama E, Wadhwa R, Kaur K *et al.* (2004) Identification of metastasis-related genes in a mouse model using a library of randomized ribozymes. *J Biol Chem* 279:38083–6

Tada A, Pereira E, Beitner-Johnson D *et al.* (2002) Mitogen- and ultraviolet-B-induced signaling pathways in normal human melanocytes. *J Invest Dermatol* 118:316–22

Vig M, Peinelt C, Beck A *et al.* (2006) CRACM1 is a plasma membrane protein essential for store-operated Ca2+ entry. *Science* 312:1220–3

Wang Y, Deng X, Mancarella S *et al.* (2010) The calcium store sensor, STIM1, reciprocally controls Orai and CaV1.2 channels. *Science* 330:105–9

Watts SW (2010) Endothelin receptors: what's new and what do we need to know? *Am J Physiol Regul Integr Comp Physiol* 298:R254–60

Wiesner B, Roloff B, Fechner K *et al.* (2003) Intracellular calcium measurements of single human skin cells after stimulation with corticotropin-releasing factor and urocortin using confocal laser scanning microscopy. *J Cell Sci* 116:1261–8

Worley PF, Zeng W, Huang GN *et al.* (2007) TRPC channels as STIM1-regulated store-operated channels. *Cell Calcium* 42:205–11

Yada Y, Higuchi K, Imokawa G (1991) Effects of endothelins on signal transduction and proliferation in human melanocytes. *J Biol Chem* 266:18352–7

Yanagisawa M, Kurihara H, Kimura S *et al.* (1988) A novel potent vasoconstrictor peptide produced by vascular endothelial cells. *Nature* 332:411–5

Yang S, Zhang JJ, Huang X-Y (2009) Orai1 and STIM1 are critical for breast tumor cell migration and metastasis. *Cancer Cell* 15:124–34

Zbytek B, Wortsman J, Slominski A (2006) Characterization of a ultraviolet B-induced corticotropin-releasing hormone-proopiomelanocortin system in human melanocytes. *Mol Endocrinol* 20:2539–47

Zhang SL, Yeromin AV, Zhang XH *et al.* (2006) Genome-wide RNAi screen of Ca(2+) influx identifies genes that regulate Ca(2+) release-activated Ca(2+) channel activity. *Proc Natl Acad Sci USA* 103:9357–62

Zhang SL, Yu Y, Roos J *et al.* (2005) STIM1 is a Ca2+ sensor that activates CRAC channels and migrates from the Ca2+ store to the plasma membrane. *Nature* 437:902–5

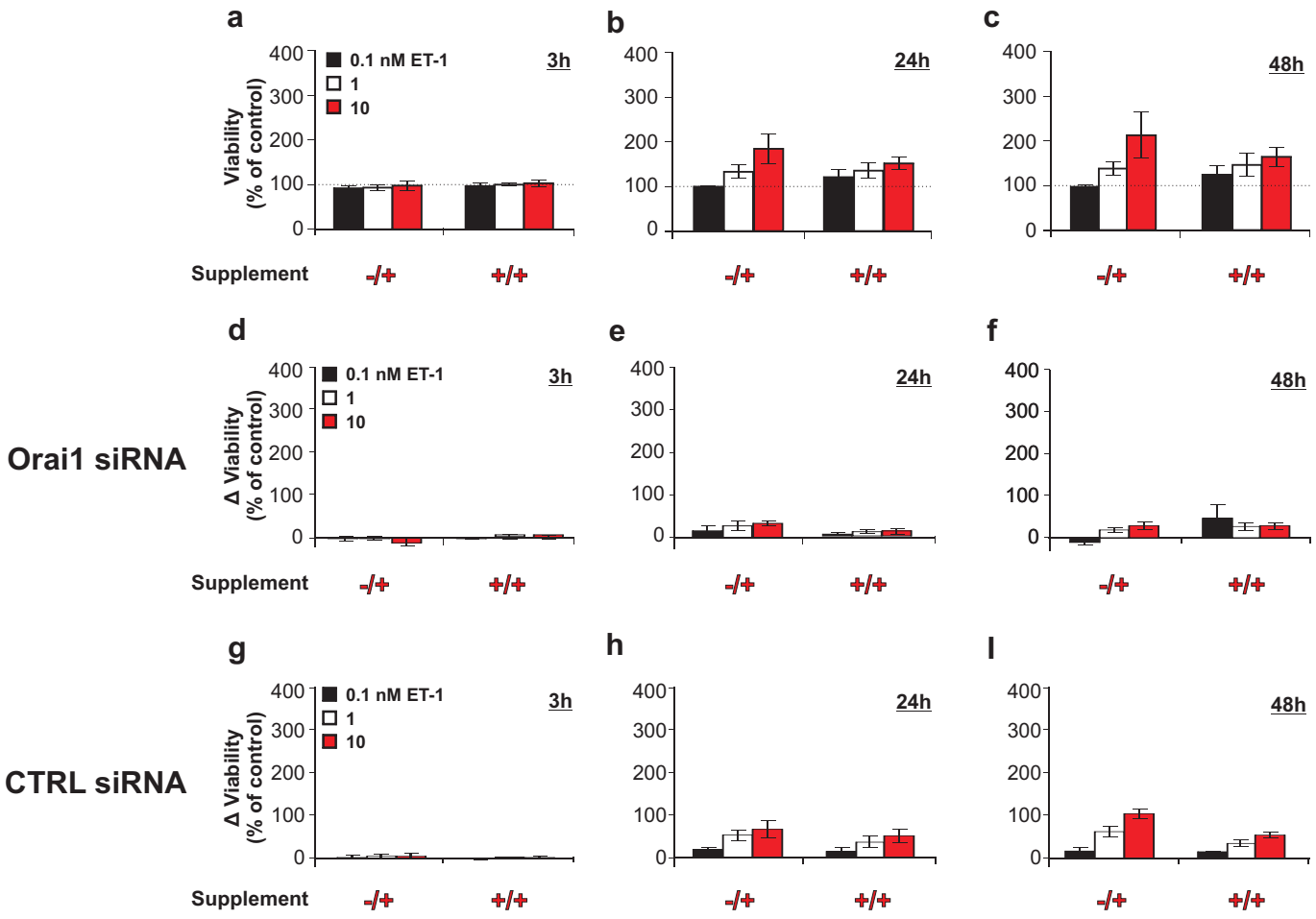

Figure S1. The role of ORAI1 in ET-1-induced melanocyte viability in differentially supplemented growth media

(a-c) Relative melanocyte viability in (-/+) and (+/+) growth medium, 3h (a), 24h (b) and 48h (c) following stimulation with 0.1, 1 and 10 nM ET-1; n=5. Results are presented as % of control (100%, without ET-1). (d-i) Change in the ET-1-induced increase in viability of melanocytes treated with O1siRNA (d-f) and CTRLsiRNA (g-i) in (-/+) and (+/+) growth medium, 3h (d), 24h (e) and 48h (f) following stimulation with 0.1, 1 and 10 nM ET-1; n=7. Measurements with ET-1 were evaluated as % of control (100%, without ET-1). To isolate the effect of ORAI1 on ET-1-induced increase in viability, 100% (value without ET-1) was subtracted from all values in panel d-i. Error bars indicate means ± SEM.